

In-Flight Thermal Performance of the OCO-2 Instrument

Arthur Na-Nakornpanom[1], Richard A.M. Lee[2] and Lars Chapsky[3]
Jet Propulsion Laboratory, California Institute of Technology, Pasadena, CA, 91109

The Orbiting Carbon Observatory-2 (OCO-2), launched on July 2, 2014, continues to operate nominally after successfully completing its primary mission of two years in space. It is hoped that, following a Senior Review and proposal phase, NASA will fund a two year extended mission, which would start in June 2017. The thermal design provides three temperature zones required by the instrument, specifically at 120 K, 267 K and 297 K. A single-stage pulse tube cryocooler provides refrigeration to three focal plane arrays to 120 K, via a high conductance flexible thermal strap. A variable conductance heat pipe (VCHP) based heat rejection system transports waste heat from the instrument, located inside the spacecraft, to the space-viewing radiators, providing tight temperature control of the spectrometer optics to 267 K, and maintains the electronics and cryocooler at 297 K. Soon after entering the A-Train on August 3, 2014, the optics and focal planes were cooled to their operating temperatures. Ice contamination of the cryogenic surfaces led to increased cryocooler loads and drove the need for two focal plane decontamination cycles between September 2014 and October 2014. A decrease in the radiometric gain of the O_2 A-Band channel led to five additional focal plane decontamination cycles, between January 2015 and February 2017, and is now the primary driver of decontamination cycles. This paper provides a general overview of the thermal and cryogenic system design and reviews the in-flight thermal performance for the mission.

Nomenclature

AFE	=	Analog Front-End Electronics
AFT	=	Allowable Flight Temperature
AR	=	Anti-Reflection
ATK	=	Alliant Techsystems
ATS	=	Absolute Time Sequence
BCA	=	Baffle Calibration Assembly
BOL	=	Beginning of Life
CCE	=	Cryocooler Control Electronics
CCIE	=	Cryocooler Interface Electronics
CSS	=	Cryogenic Subsystem
DP	=	Digital Processor
EOL	=	End of Life
FPA	=	Focal Plane Array
HEC	=	High Efficiency Cryocooler
HRS	=	Heat Rejection System
MLI	=	Multi Layer Insulation
NGAS	=	Northrop Grumman Aerospace Systems
OBA	=	Optical Bench Assembly
PIA	=	Primary Instrument Assembly
REM	=	Remote Electronics Module
SAA	=	South Atlantic Anomaly
SPC	=	Solar Polar Calibration

[1] Thermal Engineer, Cryogenic Systems Engineering Group, 4800 Oak Grove Drive, Mailstop 157-316, Pasadena, CA, 91109.
[2] Technologist, Cryogenic Instrument and Technology Development Group, 4800 Oak Grove Drive, Mailstop 79-24, Pasadena, CA, 91109.
[3] Systems Engineer, Advanced Optical Instruments Group, 4800 Oak Grove Drive, Mailstop 321-351, Pasadena, CA, 91109.

I. Introduction

THE Orbiting Carbon Observatory-2 (OCO-2) instrument, designed and built by the Jet Propulsion Laboratory (JPL) for NASA, incorporates three co-boresighted, high-resolution grating spectrometers, designed to measure the near-infrared absorption of reflected sunlight by carbon dioxide and molecular oxygen. The instrument's primary science objective is to collect space-based global measurements of atmospheric carbon dioxide with the precision, resolution, and coverage needed to characterize sources and sinks on regional scales (> 1000 km). In addition, OCO-2 quantifies carbon dioxide variability over the seasonal cycles. These measurements improve our ability to forecast CO_2 induced climate change. OCO-2 flies in a sun-synchronous, near-polar orbit at an inclination of 98.1 degrees, mean altitude of 705 kilometers, 99 minute orbit period with an ascending node crossing the equator at 1:36 PM Mean Local Time (MLT). Near-global coverage of the Earth is provided in a 16-day (233-orbit) ground-track repeat cycle. A detailed description of OCO-2 and its science capabilities can be found at https://oco.jpl.nasa.gov/. An artist's conception of the OCO-2 spacecraft flying at the head of a group of Earth-orbiting satellites known as the A-Train, with related carbon cycle science objectives, is shown in Figure 1. The spacecraft on orbit with all of its external MLI is shown in Figure 2.

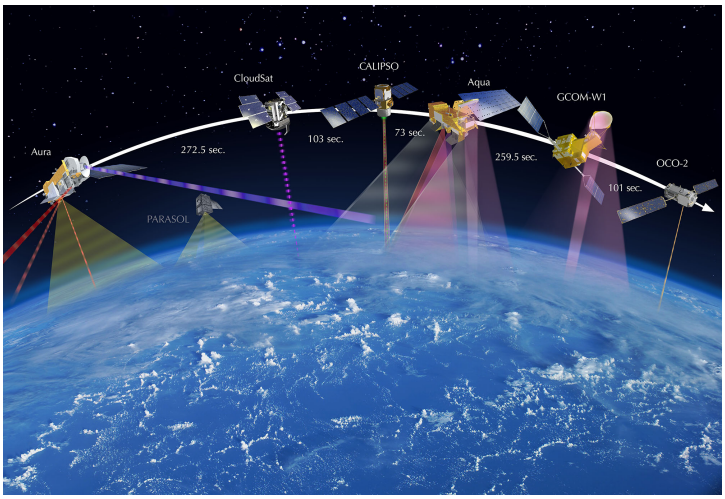

Figure 1. NASA's A-Train Constellation on orbit.

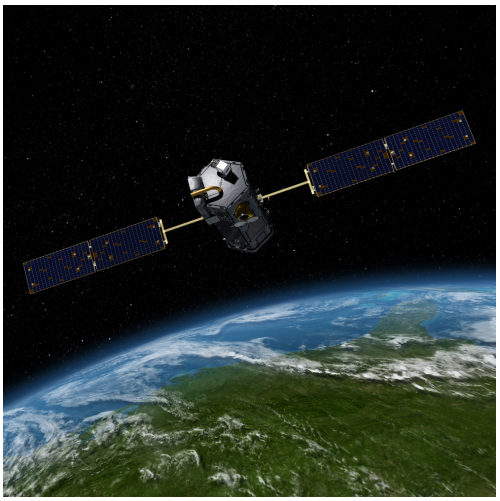

Figure 2. Artist's Rendition of OCO-2.

II. Instrument Description

The OCO-2 instrument is integrated on the LEOStar-2 spacecraft bus as shown in Figure 3. Isometric views of the OCO-2 instrument components and primary instrument assembly (PIA) are shown in Figures 4 and 5. The LEOStar-2 spacecraft bus, provided by Orbital Sciences ATK, is made primarily of aluminum honeycomb panels that form a hexagonal structure approximately 1 meter in diameter and 2 meters tall. The Earth-viewing honeycomb panels structurally support and remove waste heat from spacecraft components and instrument electronics. The REM, CCIE and CCE electronics modules are mounted on the spacecraft bus panels. A set of momentum wheels onboard the spacecraft points the instrument telescope in three primary observatory operating modes: directly downwards towards the Earth in Nadir Mode, near the subsolar point in Glint Mode and at specific locations on the Earth in Target Mode.

The heart of the OCO-2 instrument is three high-resolution diffraction grating spectrometers that measure the gas concentrations at three wavelength bands (0.76 µm O_2 A-band, 1.60 µm Weak CO_2, and 2.06 µm Strong CO_2) from sunlight reflected off the Earth's continents and oceans through a column of air in the atmosphere. By measuring CO_2 concentrations over time at the same location, OCO-2 is able to track sources and sinks on regional scales. To reduce thermally induced measurement errors, the one hybrid visible silicon (HyViSI) and two mercury cadmium telluride (HgCdTe) focal plane arrays (FPAs) must remain at a low and stable temperature. The three FPAs are cooled to ~120 K, via a flexible aluminum thermal link, from a single stage linear pulse tube cryocooler, which maintains its cold block at 110 K.

The waste heat from the cryocooler and Analog Front End (AFE) electronics are removed by means of a heat rejection system (HRS) that utilizes two VCHPs and a space viewing radiator. A second similar HRS is used to provide cooling for the spectrometer.

Figure 3. Orbiting Carbon Observatory (OCO-2).

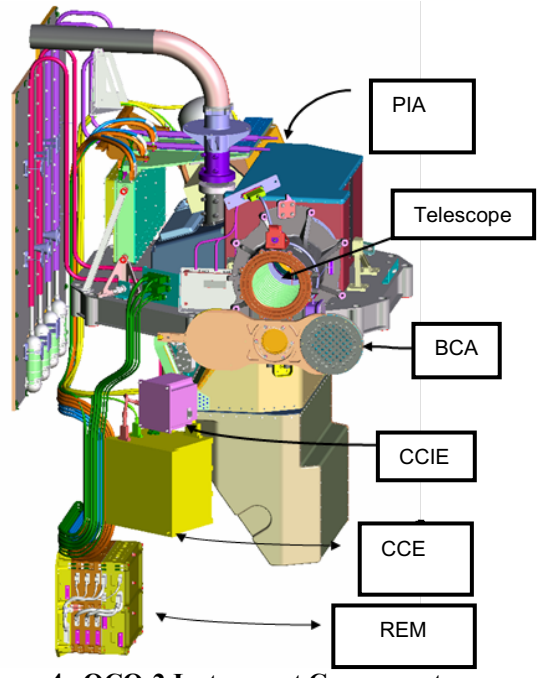

Figure 4. OCO-2 Instrument Components.

The instrument deck structure which mounts to the spacecraft provides support for the entire instrument excluding the HRS. The HRS is supported by kinematic mounting to the spacecraft bus panel. The instrument envelope is 1.0 m × 1.0 m × 1.2 m without the HRS and fits inside the spacecraft bus. The instrument mass and average operating power are 130 kg and 131.5 W, respectively.

III. Spacecraft Environment

The key thermal design drivers for the instrument are as follows:

- Orbit parameters: sun-synchronous, 705 km altitude, 1:36 PM ascending node, 98.1 degree orbit inclination.
- Spacecraft interface temperatures: 0/+40°C for science and -15/+50°C during survival mode.
- Heat transfer to the spacecraft is limited to less than 10W, which includes radiation and conduction heat transfer.
- Survival heater power allocation is 40W. This is 30% of the allocated operational average power.

The environmental parameters, and conditions of each spacecraft state, defining the bounding thermal mission environments, including spacecraft attitudes and the solar vector to orbit plane (beta) angle are shown in Table 1. During Glint mode, the spacecraft slews to follow the glint of reflected sunlight off the Earth's surface, which produces the worst-case hot environmental thermal loading. During Nadir mode, the instrument telescope remains nadir-pointed, and minimum environmental thermal loading occurs.

Table 1. OCO-2 orbit parameters.

Parameter	Hot Science	Cold Science	Extreme Cold
Mode	Glint	Nadir	Survival
Beta Angle	11°	28°	28°
SC Orientation	Glint pointing	Nadir pointing	HRS Radiators pointing towards space
Solar Flux	1420 W/m^2	1290 W/m^2	1290 W/m^2
Albedo	0.375	0.275	0.275
Earth IR	243 W/m^2	222 W/m^2	222 W/m^2

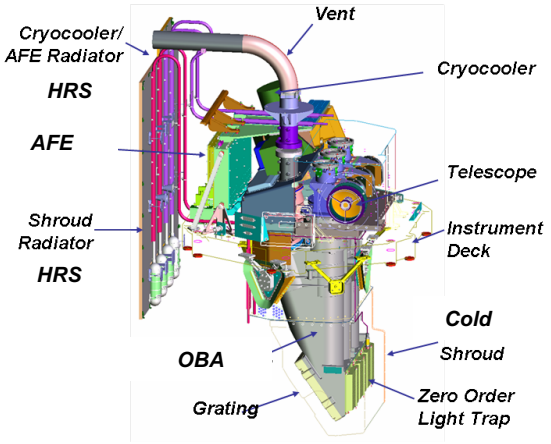

Figure 5. OCO-2 Primary Instrument Assembly.

Table 2. Allowable flight temperature requirements.

	Allowable Flight Temperatures (°C)			
	Non-Op	Operating		
	Survival	Orbit Variation	Gradient	Design
PIA	-15/+50			0/40
FPA	-168/+35	1		-168/-148
AFE	-15/+50	5		10/25
OBA	-20/+35	0.3	5	-10/0
REM	-15/+50			0/40
BCA	-15/+55			0/55
HRS	-100/+50			-100/+35
HEC	-10/+35			0/30
CCE	-20/+50			0/40
CCIE	-20/+50			0/40

IV. Thermal Design Requirements

Spacecraft thermal requirements dictated that the instrument thermal control be independent of the observatory. The instrument exterior is covered with MLI blankets and low conductance structural mounts are used to provide the required thermal isolation of the instrument from the spacecraft bus. To reject the instrument power dissipation, the instrument makes use of the spacecraft radiators, as well as HRS radiators mounted via low thermal conductance mounts on the outside of the spacecraft. MLI blanketing is applied to the back of the HRS radiators to minimize radiation heat transfer with the spacecraft panel.

The instrument temperature requirements are listed in Table 2. Instrument average power dissipation for all components is listed in Table 3. Note that the FPA and OBA temperatures are the driving thermal design requirements.

V. Thermal Control System

The instrument thermal design focuses on three main thermal control zones; 1) AFE, Cryocooler, CCIE, CCE and REM temperature zone at 297 K, 2) FPA temperature zone at 120 K, and 3) OBA temperature zone at 267 K. The REM, CCIE and CCE use the spacecraft provided 297 K zone to dissipate their waste heat.

The 120 K zone is provided with a single stage pulse tube cryocooler as shown in Figure 6. The cryocooler is the Northrop Grumman Aerospace Systems (NGAS) High Efficiency Cryocooler (HEC). Ref. 1 provides a description of the OCO-2 cryocooler system development and qualification test phases at NGAS and JPL, as well as integration and testing of the cryocooler system at both the instrument and observatory levels.

Table 3. Equipment average power dissipation.

	Component	Avg. Power (W)
AFE/ Cryocooler Radiator	Cryocooler	39.6
	AFE	20.0
	VCHP Reservoir Heaters	5.6
Shroud Radiator	VCHP Reservoir Heaters	7.6
Spacecraft Radiators	REM	30.4
	CCE	19.5
	CCIE	1.8
	Calibration Door Motor	7.0
Total Power Dissipation		**131.5**

The cryogenic subsystem (CSS), as shown in Figure 7, provides the interface between the three FPAs and the HEC. The CSS consists of three subassemblies, one for each FPA, and a flexible aluminum foil thermal link that connects each subassembly to the HEC. Each subassembly provides a mounting location for an FPA, while thermally isolating each FPA from the instrument optical bench and thermally coupling the FPAs to the HEC cold block. The FPA mounts consist of reentrant tri-fold G10 fiberglass/epoxy tube construction and MLI to minimize parasitic heat loads on the FPAs. With the HEC cold block controlled to 110 K, the CSS maintains the three FPAs near the desired temperature of 120 K.

The cryogenic surfaces of the FPAs, the flexible

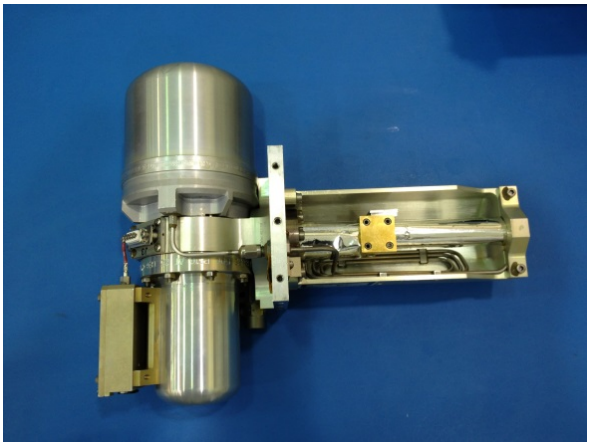

Figure 6. NGAS High Efficiency Cryocooler (HEC).

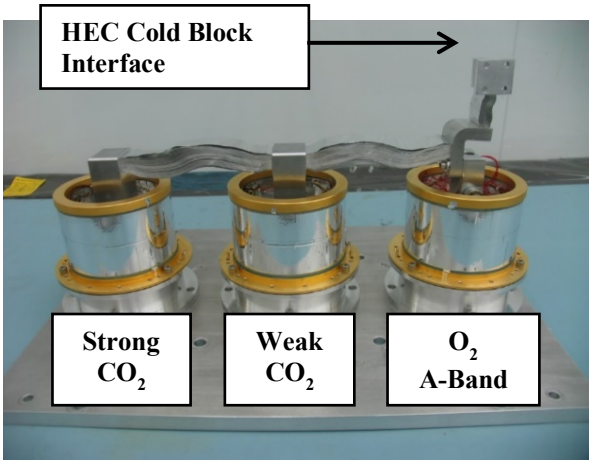

Figure 7. Cryogenic Subsystem (CSS).

thermal link and the cryocooler cold block are wrapped with MLI. MLI used in cryogenic systems absorbs water in ambient conditions. Desorption of water in vacuum is on the order of days to weeks. The freezing of water on cold surfaces increases emissivity, and consequently, parasitic radiative heat loads increase. This potentially increases the total heat load on the cryocooler such that the cryocooler can no longer provide sufficient refrigeration to maintain the required FPA temperatures within the cryocooler power allocation. Also, as ice frost accumulates on the FPAs, it progressively degrades their radiometric performance (see section VI-C). A decontamination heater on the cryocooler thermal strap allows warm up of the cold surfaces including the FPAs to defrost and drive away the water.

During launch, ascent and decontamination cycles, the outgassing particles are driven out into the instrument shroud volume due to its lower pressure (~10^{-7} torr). A large aluminum vent pipe (63.5 mm in diameter, 762 mm in length) above the OCO-2 instrument provides a flow channel between the instrument shroud volume and space. The contamination vent port exits the spacecraft and makes a 90° bend to vent away from the HRS radiators. Because the pressure in the instrument shroud volume is significantly higher than outside the spacecraft (~10^{-10} torr), the pressure differential between the two volumes provides the driving force to cause the gas particles to flow through the vent pipe. Thus, the outgassing particles from the surfaces within the shroud eventually find their way out to space.

The shroud HRS utilizes two VCHPs and a space viewing radiator to provide cooling for the cold shroud surrounding the spectrometer. The spectrometer is cooled by radiation heat transfer to the cold shroud. The radiation heat transfer helps to isothermalize the all-aluminum spectrometer. The VCHPs use aluminum axial groove extrusions and a stainless steel reservoir, with ammonia as the working fluid. An inertia weld bi-metallic aluminum to stainless steel transition joins the condenser to its non-condensable gas reservoir. Both the evaporator and condenser sections are single-sided heat input designs. The condenser sections of the VCHPs are bonded and fastened to the radiator, and the evaporator sections are attached to the cold shroud with a bolted interface. A closed-loop heater controller, with the heater located at the reservoir and a temperature sensor at the evaporator, maintains the OBA temperature at ~267 K. When the observatory is in survival mode, the instrument is off and the VCHPs are shut down to thermally decouple the components from the radiators. Table 4 shows the thermo-optical surface properties for the HRS radiators and MLI[2].

The OBA was constructed from a single aluminum casting for good isotropic properties and high thermal conductivity in order to achieve tight dimensional stability and maintain its temperature gradient to be less than 5 K. The OBA is mounted to the instrument deck structure with three low conductance struts. The cold shroud is constructed with aluminum sheet metal panels and rivets for fastening panels together. This aluminum cold shroud provides in-plane conductance to transfer the heat from the OBA with a suitable temperature gradient. MLI blankets completely surround the cold shroud to minimize radiation heat transfer to the spacecraft.

Table 4. Instrument thermo-optical surface properties.

Item	Surface Type	Surface Properties	
		BOL (α/ε)	EOL (α/ε)
White Paint	HRS Radiators	0.18/0.86	0.30/0.86
Aluminized Kapton	External MLI	0.39/0.73	0.55/0.73
15 layer Mylar	Internal MLI effectiveness	0.025	0.035

The waste heat from the cryocooler and AFE are removed by a second, similar HRS. The evaporator sections of the VCHPs are attached to an aluminum thermal plane, which interfaces to the cryocooler and AFE. A closed-loop heater controller, with the heater located at the reservoir and a temperature sensor at the evaporator, controls the cryocooler heat rejection temperature to within 300 K ± 2.5 K, and the AFE temperature to within 293 K ± 2.5 K.

The radiator panels are constructed using an aluminum honeycomb core structure with thin aluminum high conductivity facesheets. The radiators are painted white for high heat rejection and to minimize absorbed solar flux. Both HRS radiators were designed with fin efficiencies exceeding 0.85. The orientation of the radiators are always parallel to the sun vector to avoid sun exposure.

A detailed description of the thermal design of the instrument is found in Ref. 3.

VI. In-Flight Thermal Performance

A. Initial In-Flight Performance

Immediately following launch (July 2, 2014), the instrument survival heaters were enabled in the following order:

- Calibration door motor survival heater: Launch + 2 hours
- AFE/Cryocooler VCHP survival heater: Launch + 4 hours
- BCA survival heater: Launch + 9 hours
- CCE survival heater: Launch + 16 hours

The instrument REM and AFE were powered on at launch plus 21 hours. At launch plus 30 hours, the observatory transitioned from Survival Mode to Nadir Mode, and the instrument decontamination heaters were powered on to heat the FPAs and OBA to 300 K. The CCE was powered on during day 5 (July 6, 2014) to verify the health of the cryocooler system and complete the instrument initial checkout. The OCO-2 instrument was subjected to a 32 day decontamination period to allow time for the moisture in the instrument structure and MLI to diffuse away from the CSS, into the instrument shroud volume, and out through the aluminum vent pipe into space. The initial orbit altitude after launch was ~692 km and after a series of delta-V maneuvers, performed over 25 days, the spacecraft reached its final altitude of 705 km on day 33 (August 3, 2014).

To end the decontamination period, and prepare the instrument for cool down, the instrument decontamination heaters were turned off on day 34 (August 4, 2014). On day 35 (August 5, 2014), the HEC compressor was powered on. On day 36 (August 6, 2014), the instrument entered operational mode and the observatory began a data collection cycle where it alternated between 16 days in Glint Mode and 16 days in Nadir Mode. Figures 8 to 13 show the in-flight thermal performance.

As seen in Figure 8, the initial water ice accumulation rate resulted in the HEC drive level increasing at a rate of 0.62% per day. As ice accumulates the FPAs drift up in temperature while the HEC cold head maintains its temperature setpoint. Due to the science requirement of maintaining the mean of the strong and weak CO_2 FPA temperatures at ~ 120 K, the HEC cold head setpoint needs to be adjusted downwards periodically, as shown in Figure 9, due to the FPAs drifting out of range (green horizontal band).

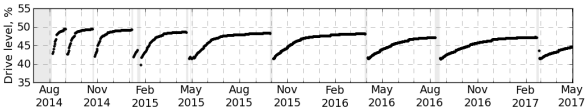

Figure 8. In-Flight Cryocooler Drive Level.

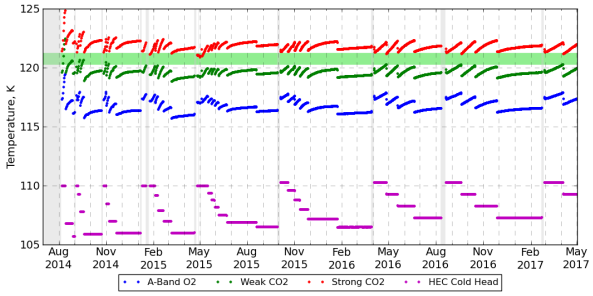

Figure 9. In-Flight Cryocooler Cold Block and FPA Temperatures.

B. De-Icing Results

The initial 32-day outgassing period was not sufficient to remove all of the water vapor from the instrument. Prior to launch, it was recognized that science measurements would need to be interrupted periodically as a result of water ice cryodepositing onto the cold surfaces of the CSS[4]. The water contamination increases the thermal heat load, which in turn leads the cryocooler motor drive level to approach its user-programmable maximum limit of 50%. Due to limitations with the spacecraft bus power budget, the HEC is limited to a maximum of 48 W compressor power, which is equivalent to 50% motor drive level.

With the HEC drive level increasing at a rate of 0.04% per day, the 50% limit would have been reached by day 70. The first de-ice cycle was started on day 61 (August 31, 2014), with the turning off of the HEC, followed by turning on the FPA decontamination heater and taking 6 hours to reach the target temperature of 285 K, for the FPAs, in order to drive off any accumulated water out through the instrument vent pipe. After two days of de-icing, the decontamination heater was turned off on day 63 (September 2, 2014). After powering on the HEC, it took ~12 hours for the cold head to reach 110 K. The entire decontamination cycle, from when the cryocooler was shut down to when the FPAs returned to their steady-state operating temperatures, took 72 hours. A detailed description of the in-flight performance of the cryocooler subsystem is found in Ref. 5.

Figure 9 shows the HEC cold head and FPA temperatures for the first 33 months of cryocooler operation. After each de-ice cycle, the cold head setpoint needs to be decreased in steps in order to maintain the FPAs at ~ 120 K. The second de-ice cycle was started on day 114 (October 23, 2014) again due to projections that the 50% drive limit would soon be reached. After two days of de-icing, the decontamination heater was turned off and the HEC was restarted. Figure 8 shows that the level of icing has decreased over time after each de-ice cycle, and the HEC motor drive level now consistently remains well below 50%.

C. Radiometric Gain Degradation in O_2 A-Band FPA

The observation of decreasing responsivity of the O_2 A-band FPA (gradually decreasing to ~95%) has been attributed to accumulation of a thin layer of ice (< 100 nm) on the FPA and a concomitant reduction in the efficiency of the anti-reflection (AR) coating. After the second de-ice cycle, the requirement to de-ice was no longer driven by the 50% HEC motor drive limit, but now driven by gain degradation in the O_2 A-band FPA. There have been five gain degradation-driven de-ice cycles starting on day 189 (January 6, 2015), day 293 (April 20, 2015), day 454 (September 28, 2015), day 636 (March 28, 2016), and day 966 (February 21, 2017). The FPA performance has been almost fully restored after each de-ice cycle (note, a small portion of the observed degradation is attributed to permanent instrument degradation).

Note that the O_2 A-Band FPA is strongly affected by thin ice layers because it has a high intrinsic reflectance, and uses an AR coating with a refractive index more similar to water ice (1.33) than the optimum AR coating (1.98). The other two FPAs are much less sensitive to thin layers of water ice because they have a lower intrinsic refractive index (2.65) and an AR coating with a better optimized refractive index (~2.0).

D. Cryocooler Accelerometer Overload Trip

The HEC unexpectedly tripped off on day 200 (January 17, 2015) due to an accelerometer overload fault. The accelerometer overload detector is intended to protect the HEC against over-stroking. It does not differentiate between internal cooler vibration and external vibration, and can be false alarmed by external mechanical noise. This type of trip had been observed during cryocooler and instrument ground testing, where the cause was attributed to external sources such as vibrating heat exchanger chiller lines or movement of ground support equipment. In the interest of returning OCO-2 back to science operating mode, it was determined that there was no risk to powering on the HEC with the accelerometer overload trip function remaining enabled. This trip event provided the opportunity to perform a de-ice cycle. After six days of de-icing, the HEC was powered on day 206 (January 23, 2015) and the cryocooler system has operated normally to date.

However, the root cause investigation and corrective action remained open, due to the risk that a similar trip could reoccur. Analysis of cryocooler telemetry showed that the HEC had been operating normally up to the time of the event. There were no unique instrument or spacecraft activities at the time of the trip, and the space environment was normal.

After a thorough investigation, the root cause could not be identified, and the event was deemed to be a false trip. The CCE provides several layers of protection against over-stroke: asynchronous time-domain accelerometer overload detection, synchronous frequency-domain individual harmonic over-vibration detection, motor over-current detection and motor drive limit. Since the cryocooler is operating at a low fraction of its maximum stroke, and due to the other layers of protection in place, it was decided to implement the corrective action of disabling the accelerometer overload detector on day 306 (May 3, 2015) to eliminate the risk of future false alarms. There have been no subsequent cryocooler faults of any kind to date.

E. Instrument Trips

The spacecraft fault detection system unexpectedly tripped off the instrument digital processors (DPs) and analog front-end electronics (AFE) on day 299 due to an error in the observatory absolute time sequence (ATS), which is used to command the observatory autonomously. The ATS was expected to open the instrument telescope door before exiting eclipse with nominal fault protection in place, allowing the instrument to see the sunlit Earth.

However, the ATS incorrectly had solar polar calibration (SPC) fault protection enabled, thus when OCO-2 exited eclipse with the door open, an SPC fault occurred, resulting in an unnecessary shut-down of the instrument DPs and AFE for protection. It was therefore necessary to power cycle the instrument, in order to reset it to its nominal state, which provided the opportunity to perform another de-ice cycle. After one day of de-icing, the HEC was powered on during day 302 (April 29, 2015).

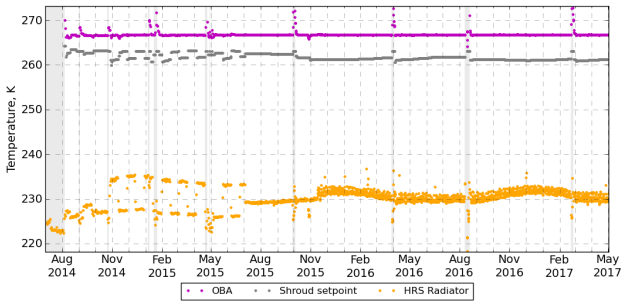

Figure 10. In-Flight OBA and Shroud VCHP Temperatures.

However, as the instrument was recovering on day 302, the spacecraft fault detection system again unexpectedly tripped off the instrument DPs and AFE due to a redundant fault protection setting in the instrument power cycle sequence that was overlooked. Again, the instrument fault protection was incorrectly enabled and the DPs and AFE powered off for protection. The instrument had to be power cycled again, providing another opportunity to perform a de-ice cycle. After one day of de-icing, the HEC was powered on during day 306 (May 3, 2015).

The spacecraft fault detection system shut down the instrument on day 771 (August 10, 2016) due to an unexpected instrument REM power-on reset over the South Atlantic Anomaly (SAA). During an instrument power-on reset, the REM reboots itself. As the REM recovers, there is a delay with valid instrument telemetry. The spacecraft continues to monitor the instrument telemetry while the REM is recovering, with nominal instrument fault protection enabled. Due to persistent bad telemetry from the instrument, the spacecraft fault detection triggered commands to shut down the instrument. This event provided an opportunity to perform another de-ice cycle. After six days of de-icing, the HEC was powered on during day 780 (August 19, 2016). There have been no subsequent instrument faults of any kind to date.

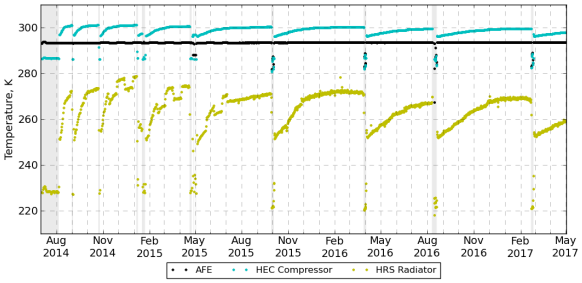

Figure 11. In-Flight Cryocooler and AFE Temperature.

F. Heat Rejection System Performance

During the first year of the OCO-2 mission from July 2014 to July 2015, it was difficult to maintain the OBA at the nominal 267 K as shown in Figure 10 due to the observatory Nadir/Glint mode cycling every 16 days. The shroud VCHP heater control setpoint needed a ~ ± 1 K adjustment after each Nadir/Glint mode change. In order to acquire valid science data over land and ocean every day, rather than every 16 days, OCO-2 adopted an alternating Nadir/Glint mode orbit scheme starting on July 3, 2015. The temperature data from July 3, 2015 onward show improved temperature control of the OBA, with only minor (~ ± 0.1 K) adjustments required for the shroud VCHP heater controller. On November 12, 2015, the alternating Nadir/Glint mode was modified to provide more Glint orbits over the oceans (called the optimal orbit scheme), with minimal impact to thermal management.

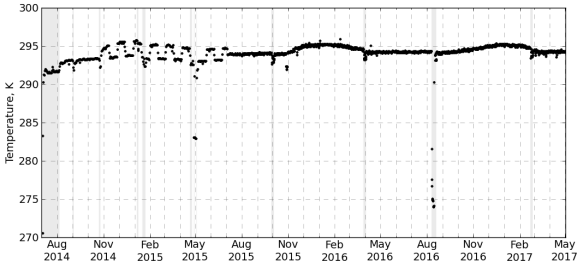

Figure 12. In-Flight REM Temperature.

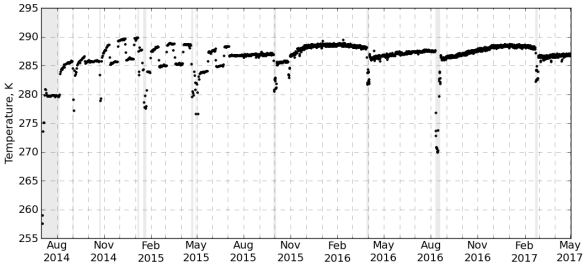

Figure 13. In-Flight CCE Temperature.

The HRS for the cryocooler and AFE has performed exceptionally well and maintained the HEC and AFE within their nominal temperature range as shown in Figure 11. When the cryocooler is turned on, its baseplate reaches a maximum temperature of 303 K during cooldown. The baseplate is maintained at an average temperature of 300 K when the cryocooler is in stable operation. When the cryocooler is turned off, the HRS

maintains the baseplate at an average temperature of 286 K. The heater control system on the VCHP HRS maintains the cryocooler rejection temperature variation to ~ 0.6 K p-p while the radiator temperature varies by ~ 20 K p-p.

Figures 12 and 13 detail the REM and CCE heat rejection temperature variation. The CCE endured a cold start at 253 K on day 5. The two planned instrument power off/on cycles in late April 2015 and early May 2015 were performed in back-to-back orbits, to prevent the instrument from reaching survival temperatures, thus the CCE temperature was maintained well above 253 K. The effect of the transitions between the 16 day Nadir and Glint Mode cycle on the spacecraft panels are clearly seen on the REM and CCE prior to July 3, 2015. After the start of the Nadir/Glint mode alternating orbit scheme, and later optimal orbit scheme, the REM and CCE temperatures exhibit a smoother trend.

VII. Conclusion

The OCO-2 thermal and cryogenic system development was important to the success of the OCO-2 instrument development and focused on integrating thermal and cryogenic technologies to maximize the overall instrument performance. This was a highly collaborative activity involving contractual support from ATK Space Systems in Beltsville, Maryland, Utah State University, Space Dynamics Laboratory in Logan, Utah, and Northrop Grumman Aerospace Systems in Redondo Beach, California. The overall thermal and cryogenic systems have performed exceptionally well to date. The ice contamination rate on the FPAs and cryogenic surfaces has decreased over time such that de-icing cycles are now only performed once every six months. The thermal and cryogenic systems are performing to specification, have enabled OCO-2 to meet its primary mission science objectives, and are expected to continue should there be an extended mission.

Acknowledgments

The authors would like to thank the JPL OCO-2 team, as well as the subcontractors that have contributed to the success of the OCO-2 instrument and observatory, including Northrop Grumman Aerospace Systems in Redondo Beach, California, and Orbital Sciences ATK in Dulles, Virginia and Gilbert, Arizona. The authors would especially like to recognize the support of the OCO-2 Project Manager, Patrick J. Guske.

These data were produced by the OCO-2 Project at the Jet Propulsion Laboratory, California Institute of Technology, and obtained from the OCO-2 data archive maintained at the NASA Goddard Earth Science Data and Information Services Center.

References

[1]Na-Nakornpanom, A., Johnson, D.J., and Naylor, B.J., "OCO-2 Cryocooler Development, Integration and Test," *18th International Cryocooler Conference*, Syracuse, NY, Cryocoolers 18, ICC Press, 2014, pp. 105-114

[2]Gilmore, D.G., *Spacecraft Thermal Control Handbook*, Volume I: Fundamental Technologies, 2nd ed., Aerospace Press, 2002.

[3]Rivera, J.G., Rodriguez, J.I., and Johnson, D.J., "Development of the Orbiting Carbon Observatory Instrument Thermal Control System," *International Conference on Environmental Systems*, San Francisco, CA, SAE, 2008.

[4]Ross, R.G., "Cryocooler Load Increase Due to External Contamination of Low-ε Cryogenic Surfaces," *12th International Cryocooler Conference*, Cambridge, MA, Cryocoolers 12, Plenum, 2002, pp. 727-736

[5]Na-Nakornpanom, A., Naylor, B.J., and Lee, R.A.M., "In-Flight Performance of the OCO-2 Cryocooler," *55th Cryogenic Engineering Conference*, Tucson, AZ, Vol. 101, IOP, 2015

[6]Rodriguez, J.I., Na-Nakornpanom, A., Rivera, J.G., Mireles, V., and Tseng, H., "On-Orbit Performance of the TES Instrument – Three Years in Space," *International Conference on Environmental Systems*, San Francisco, CA, SAE, 2008.